PHYSICAL REVIEW D **73,** 075015 (2006)

Single top quark production in flavor-changing Z' models

Abdesslam Arhrib,[1,2,*] Kingman Cheung,[1,3,†] Cheng-Wei Chiang,[4,5,‡] and Tzu-Chiang Yuan[3,§]

[1]*National Center for Theoretical Sciences, National Tsing Hua University, Hsinchu, Taiwan, R.O.C.*
[2]*Faculté des Sciences et Techniques, B.P 416 Tangier, Morocco.*
[3]*Department of Physics, National Tsing Hua University, Hsinchu, Taiwan, R.O.C.*
[4]*Department of Physics, National Central University, Chungli, Taiwan 320, R.O.C.*
[5]*Institute of Physics, Academia Sinica, Taipei, Taiwan 115, R.O.C.*

(Received 28 February 2006; published 28 April 2006)

In some models with an extra $U(1)$ gauge boson Z', the gauge couplings of the Z' to different generations of fermions may not be universal. Flavor mixing in general can be induced at the tree level in the up-type and/or down-type quark sector after diagonalizing their mass matrices. In this work, we concentrate on the flavor mixing in the up-type quark sector. We deduce a constraint from $D^0 - \bar{D}^0$ mixing. We study in detail single top-quark production via flavor-changing Z' exchange at the Large Hadron Collider (LHC) and the International Linear Collider (ILC). We found that for a typical value of $M_{Z'} = 1$ TeV, the production cross section at the LHC can be of the order of 1 fb. However, the background from the standard model single top-quark production makes it difficult to detect the flavor-changing Z' signal unless a decent charm tagging method is implemented. On the other hand, at the ILC, the production cross section at the resonance energy of $\sqrt{s} \approx M_{Z'}$ can reach a size of more than 100 fb. Even away from the resonance, the cross section at ILC is shown to be larger than the threshold of observability of 0.01 fb.

DOI: 10.1103/PhysRevD.73.075015 PACS numbers: 12.60.Cn, 14.70.Pw

I. INTRODUCTION

Searches for flavor-changing neutral currents (FCNC) have been pursued for many years. So far the sizes of FCNC in the u-c, b-s, s-d, and b-d sectors are in general agreement with the standard model (SM) predictions, namely, those given by the Cabibbo-Kobayashi-Maskawa (CKM) mechanism. In the SM, tree-level FCNC is absent in both gauge and Yukawa interactions. They can only arise from loop diagrams, such as penguin and box diagrams, and are therefore highly suppressed. Nevertheless, one-loop FCNC processes can be enhanced by orders of magnitude in some cases due to the presence of new physics, see Ref. [1] for a review. Tree-level FCNCs via some exotic gauge bosons are empirically allowed only if these bosons are sufficiently heavy or their couplings to SM particles are sufficiently small; otherwise, they would have been ruled out by current data [2–6].

However, the effects of FCNC involving the top-quark are not yet well probed experimentally, at least not by the present data. From the existing LEP and Tevatron data we have only very weak constraints on the t-q-Z and t-q-γ FCNC couplings. These constraints will not be improved any further until the operation of the Large Hadron Collider (LHC) or perhaps a future International Linear Collider (ILC) [7] is built. The goal of the paper is to analyze effects of tree-level FCNC interactions induced by an additional Z' boson on the up-type quark sector in general. In particular, we study the $t\bar{c} + \bar{t}c$ production at the LHC and ILC.

Examples of Z' arising from some grand unified theory (GUT) models are [2]:

$$Z_\psi \text{ occurring in } E_6 \to SO(10) \times U(1)_\psi,$$
$$Z_\chi \text{ occurring in } SO(10) \to SU(5) \times U(1)_\chi,$$
$$Z_\eta \equiv \cos\theta Z_\chi - \sin\theta Z_\psi, \qquad \cos\theta = \sqrt{3/8}.$$

In these examples, the SM fermions together with an additional right-handed neutrino are placed in the **16** of $SO(10)$ embedded in the **27** of E_6. One expects in such models that the Z' boson will couple universally to the three generations of fermions and thus the couplings are diagonal in the flavor space.[1] However, it is possible that exotic quarks like h and h^c in the **27** of E_6 may have their $U(1)'$ charges different from the left-handed and right-handed down-type quarks. In this case, the SM quarks will mix, leading to in general both Z- and Z'-mediated FCNCs. We note that a flavor-changing Z' boson can also arise in certain dynamical symmetry breaking models [8].

In some string models, the three generations of SM fermions are constructed differently, resulting in family nonuniversal Z' couplings to fermions in different generations. As a first step, we consider the particular case that the Z' couples with a different strength to the third genera-

*Electronic address: aarhrib@ictp.it
†Electronic address: cheung@phys.nthu.edu.tw
‡Electronic address: chengwei@phy.ncu.edu.tw
§Electronic address: tcyuan@phys.nthu.edu.tw

[1]Since the vector- and axial-vector-current interactions of Z' always couple to either two left-handed fields or two right-handed fields, the unitary rotations of the gauge eigenstates to the mass eigenstates will always preserve the diagonality of the Z' interactions if the chiral couplings are family-universal.

tion, as motivated by a particular class of string models [9]. Once we do a unitary rotation from the interaction basis to mass eigenbasis, tree-level FCNCs are induced naturally. Several works have been done regarding the FCNCs in the down-type quark sector recently [4–6]. The same can occur in the up-type quark sector too. In order to increase the predictive power of our model, we assume in this paper that the left-handed down-type sector is already in diagonal form, such that $V_{\rm CKM} = V_{uL}^{\dagger}$, where V_{uL} is the left-handed up-type sector unitary rotation matrix. Since we do not have much information about both the right-handed up-type and down-type sectors, we simply assume that their Z' interactions are family-universal and flavor-diagonal in the interaction basis. In this case, unitary rotations keep the right-handed couplings flavor-diagonal. Therefore, the only FCNCs arise in the left-handed t-c-u sector and depend on the CKM matrix elements and one additional parameter x, which denotes the strength of the Z' coupling to the third generation relative to the first two generations. Consequently, if x is an $O(1)$ parameter but not exactly equal to 1, the t-c-Z' will produce the largest FCNC effect.

Associated top-charm production at the LHC or ILC in the SM is expected to be very suppressed [10]. However, the rates enhanced by the presence of new physics such as supersymmetry (SUSY), topcolor-assisted technicolor or extended Higgs sector [11] may reach observable rates in some cases, and can then be used to probe FCNC couplings. Single top production can also proceed through the introduction of anomalous couplings: t-q-g, t-q-γ and t-q-Z [12] at both hadron and e^+e^- colliders. Such model independent analysis are useful in probing the strength of observable FCNC couplings. Many detailed studies of the Z' phenomenology have been done in recent years [2–6,13–18].

In this work, we study the capability of the LHC and the ILC to identify the t-c FCNC effect by measuring the production of $t\bar{c} + \bar{t}c$ pairs. Since most of the cross section comes from the s-channel production of the Z', these types of FCNC processes will be searched only after the Z' is discovered. The most obvious channel to discover the Z' is the Drell-Yan process at the LHC, in which a clean resonance peak can be identified in the invariant mass spectrum $M(\ell^+\ell^-)$ of the lepton-antilepton pair. Experimenters can then search for the hadronic modes with an invariant mass reconstructed at the Z' mass. Those involving the top-quark may be somewhat complicated because of the 3-jet or 1-jet-1-lepton-E_T decay products of the parent top-quark. But in principle they can be measured, though at lower efficiencies. At the LHC, however, the SM single top-quark production presents a challenging background to $t\bar{c} + \bar{t}c$ production. Unless one can efficiently distinguish the charm-quark from the bottom-quark and the other light quarks, the SM single top-quark background makes the FCNC $t\bar{c} + \bar{t}c$ process very pessimistic. There may be a slight possibility of D-tagging but it is still too early to tell its efficiency. On the other hand, an e^+e^- collider or the ILC is an ideal place to search for $t\bar{c} + \bar{t}c$ FCNC production. One can measure the ratio of the production rates for $t\bar{t}$: $t\bar{c} + \bar{t}c$: $c\bar{c}$ to identify the FCNC in the t-c sector. Also, charm tagging is considerably easier in the e^+e^- environment. At any rate, one can simply measure the $t\bar{t}$ pairs and a single top-quark plus one jet (either c or u) in the hadronic decays of the Z' boson. We will estimate the potential of this approach in this paper.

The organization of the paper is as follows. In the next section, we outline the formalism of the model. In Sec. III, we derive the current limit on the c-u transition from the D^0-$\bar{D}^0$ mixing. We calculate the production rates of various channels and estimate their detectabilities in Sec. IV. Our conclusion is presented in Sec. V.

II. FORMALISM

We follow closely the formalism in Ref. [3]. In the gauge eigenstate basis, the neutral current Lagrangian can be written as

$$\mathcal{L}_{\rm NC} = -eJ^{\mu}_{\rm em}A_{\mu} - g_1 J^{(1)\mu} Z^0_{1\mu} - g_2 J^{(2)\mu} Z^0_{2\mu}, \qquad (1)$$

where Z^0_1 is the $SU(2) \times U(1)$ neutral gauge boson, Z^0_2 the new gauge boson associated with an additional Abelian gauge symmetry. We assume for simplicity that there is no mixing between Z^0_1 and Z^0_2, then they are also the mass eigenstates Z and Z' respectively. The current associated with the additional $U(1)'$ gauge symmetry is

$$J^{(2)}_{\mu} = \sum_{i,j} \overline{\psi}_i \gamma_{\mu} [\epsilon^{(2)}_{\psi_{L_{ij}}} P_L + \epsilon^{(2)}_{\psi_{R_{ij}}} P_R] \psi_j, \qquad (2)$$

where $\epsilon^{(2)}_{\psi_{L,R_{ij}}}$ is the chiral coupling of Z^0_2 with fermions i and j running over all quarks and leptons. If the Z^0_2 couplings are diagonal but family-nonuniversal, flavor-changing couplings are induced by fermion mixing.

Z'-mediated FCNCs have been studied in detail in Ref. [4] for the down-type quark sector and their implications in B meson decays. Since such an effect may occur to the up-type quarks as well, we concentrate on this sector in this paper. For simplicity, we assume that the Z' couplings to the leptons and down-type quarks are flavor-diagonal and family-universal: $\epsilon^d_{L,R} = Q^d_{L,R}\mathbf{1}$, $\epsilon^e_{L,R} = Q^e_{L,R}\mathbf{1}$ and $\epsilon^{\nu}_L = Q^{\nu}_L \mathbf{1}$ where $\mathbf{1}$ is the 3×3 identity matrix in the generation space and $Q^d_{L,R}$, $Q^e_{L,R}$ and Q^{ν}_L are the chiral charges. On the other hand, the interaction Lagrangian of Z' with the up-type quarks is given by

$$\mathcal{L}^{(2)}_{\rm NC} = -g_2 Z'_{\mu} (\bar{u}, \bar{c}, \bar{t})_I \gamma^{\mu} (\epsilon^u_L P_L + \epsilon^u_R P_R) \begin{pmatrix} u \\ c \\ t \end{pmatrix}_I \qquad (3)$$

where the subscript I denotes the interaction basis. For definiteness in our predictions, we assume

$$\epsilon_L^u = Q_L^u \begin{pmatrix} 1 & 0 & 0 \\ 0 & 1 & 0 \\ 0 & 0 & x \end{pmatrix} \quad \text{and} \quad \epsilon_R^u = Q_R^u \begin{pmatrix} 1 & 0 & 0 \\ 0 & 1 & 0 \\ 0 & 0 & 1 \end{pmatrix}. \tag{4}$$

That is, only the left-handed couplings are family nonuniversal. The deviation from family universality and thus the magnitude of FCNC are characterized by the parameter x in the $\bar{t}_L$-t_L-Z' entry, which we take to be of $O(1)$ but not equal to 1. $Q^u_{L,R}$ are the chiral $U(1)'$ charges of the up-type quarks. The chiral charges need to be specified by the Z' model of interest.

When diagonalizing the up-type Yukawa coupling or the mass matrix, we rotate the left-handed and right-handed fields by V_{uL} and V_{uR}, respectively. Therefore, the Lagrangian $\mathcal{L}^{(2)}_{\rm NC}$ becomes

$$\mathcal{L}^{(2)}_{\rm NC} = -g_2 Z'_\mu (\bar{u}, \bar{c}, \bar{t})_M \gamma^\mu (V^\dagger_{uL} \epsilon^u_L V_{uL} P_L + V^\dagger_{uR} \epsilon^u_R V_{uR} P_R) \begin{pmatrix} u \\ c \\ t \end{pmatrix}_M \tag{5}$$

where the subscript M denotes the mass eigenbasis. With the form of ϵ^u_R assumed in Eq. (4), the right-handed sector is still flavor-diagonal in the mass eigenbasis, because ϵ^u_R is proportional to the identity matrix. However, $V^\dagger_{uL} \epsilon^u_L V_{uL}$ is in general nondiagonal. With the fact that $V_{\rm CKM} = V^\dagger_{uL} V_{dL}$ and our assumption of the down-quark sector has no mixing,

$$V_{\rm CKM} = V^\dagger_{uL}.$$

The flavor mixing in the left-handed fields is in this case simply related to $V_{\rm CKM}$, making the model more predictive. Explicitly,

$$B^u_L \equiv V^\dagger_{uL} \epsilon^u_L V_{uL} = V_{\rm CKM} \epsilon^u_L V^\dagger_{\rm CKM} \approx Q^u_L \begin{pmatrix} 1 & (x-1)V_{ub}V^*_{cb} & (x-1)V_{ub}V^*_{tb} \\ (x-1)V_{cb}V^*_{ub} & 1 & (x-1)V_{cb}V^*_{tb} \\ (x-1)V_{tb}V^*_{ub} & (x-1)V_{tb}V^*_{cb} & x \end{pmatrix} \tag{6}$$

where we have used the unitarity conditions of $V_{\rm CKM}$. It is easy to see that the sizes of the flavor-changing couplings satisfy in the following hierarchy: $|B^{tc}_L| > |B^{tu}_L| > |B^{cu}_L|$. Note that the right-handed couplings are flavor-diagonal and are of $O(1)$.

The following Z' models will be considered in this work: (i) Z' of the sequential Z model, (ii) Z_{LR} of the left-right symmetric model, (iii) Z_χ occurring in $SO(10) \to SU(5) \times U(1)$, (iv) Z_ψ occurring in $E_6 \to SO(10) \times U(1)$, and (v) $Z_\eta \equiv \sqrt{3/8} Z_\chi - \sqrt{5/8} Z_\psi$ occurring in many superstring-inspired models in which E_6 breaks directly down to a rank-5 group [19]. In the sequential Z model, the gauge coupling $g_2 = g_1$ and the chiral couplings are the same as the SM Z boson. In the other models, the gauge coupling takes on the value

$$g_2 = \sqrt{\tfrac{5}{3}} \sin\theta_{\rm w} g_1 \lambda_g^{1/2},$$

where λ_g is $O(1)$ in string-inspired models and $\theta_{\rm w}$ is the Weinberg angle. We simply choose $\lambda_g = 1$ throughout. The chiral couplings of the Z_{LR} in the left-right symmetric model is given by [19]

$$Q^i_L = -\sqrt{\frac{3}{5}} \left(\frac{1}{2\alpha} \right) (B - L)_i, \tag{7}$$

$$Q^i_R = \sqrt{\frac{3}{5}} \left(\alpha T^i_{3R} - \frac{1}{2\alpha} (B - L)_i \right), \tag{8}$$

where B and L denote the baryon and lepton numbers of the fermion i, respectively. T_{3R} is the third component of its right-handed isospin in the $SU(2)_R$ group. In the left-right symmetric model with $g_L = g_R$, the parameter α is given by

$$\alpha = \left(\frac{1 - 2\sin^2\theta_{\rm w}}{\sin^2\theta_{\rm w}} \right)^{1/2} \simeq 1.52,$$

where we have used $\sin^2\theta_{\rm w} = 0.2316$. The chiral charges for these various Z' models are compiled in Table I.

TABLE I. Chiral couplings of various Z' models.

	Sequential Z	Z_{LR}	Z_χ	Z_ψ	Z_η
Q^u_L	0.3456	−0.08493	$\frac{-1}{2\sqrt{10}}$	$\frac{1}{\sqrt{24}}$	$\frac{-2}{2\sqrt{15}}$
Q^u_R	−0.1544	0.5038	$\frac{1}{2\sqrt{10}}$	$\frac{-1}{\sqrt{24}}$	$\frac{2}{2\sqrt{15}}$
Q^d_L	−0.4228	−0.08493	$\frac{-1}{2\sqrt{10}}$	$\frac{1}{\sqrt{24}}$	$\frac{-2}{2\sqrt{15}}$
Q^d_R	0.0772	−0.6736	$\frac{-3}{2\sqrt{10}}$	$\frac{-1}{\sqrt{24}}$	$\frac{-1}{2\sqrt{15}}$
Q^e_L	−0.2684	0.2548	$\frac{3}{2\sqrt{10}}$	$\frac{1}{\sqrt{24}}$	$\frac{1}{2\sqrt{15}}$
Q^e_R	0.2316	−0.3339	$\frac{1}{2\sqrt{10}}$	$\frac{-1}{\sqrt{24}}$	$\frac{2}{2\sqrt{15}}$
Q^ν_L	0.5	0.2548	$\frac{3}{2\sqrt{10}}$	$\frac{1}{\sqrt{24}}$	$\frac{1}{2\sqrt{15}}$

Before ending this section, we quote current limits on an extra $U(1)$ gauge boson from direct searches at colliders. The most stringent limits are given by the preliminary results from CDF [20] at the Tevatron:

$$Z'_{\rm SM} > 845 \text{ GeV}, \qquad Z_\chi > 720 \text{ GeV},$$
$$Z_\psi > 690 \text{ GeV}, \quad \text{and} \quad Z_\eta > 715 \text{ GeV}.$$

In the following, we will use a typical value of $M_{Z'} = 1$ TeV unless otherwise stated.

III. CONSTRAINTS FROM D^0-$\bar{D}^0$ MIXING

A. D^0-$\bar{D}^0$ mixing in SM

To second order in perturbation, the off-diagonal elements in the neutral D meson mass matrix contain two contributions from short-distance physics. One part in-

volves $|\Delta C| = 2$ local operators from box and dipenguin diagrams [21,22] at the m_D scale, contributing to only the dispersive part of the mass matrix. Because of a severe CKM suppression in the SM, the contribution from this part is negligible. The other part involves the insertion of two $|\Delta C| = 1$ transitions, contributing to both the dispersive and absorptive parts of the mass matrix.

Since CP is a good approximate symmetry in D decays, we have the CP eigenstates $|D_\pm\rangle$ with $\mathcal{CP}|D_\pm\rangle = \pm|D_\pm\rangle$ as the mass eigenstates too. It is convenient to define

$$\Delta m_D = m_+ - m_-, \qquad \Delta\Gamma_D = \Gamma_+ - \Gamma_-, \qquad \overline{\Gamma}_D = \tfrac{1}{2}(\Gamma_+ + \Gamma_-), \tag{9}$$

and consider the dimensionless parameters

$$x_D \equiv \frac{\Delta M_D}{\overline{\Gamma}_D} \quad \text{and} \quad y_D \equiv \frac{\Delta\Gamma_D}{2\overline{\Gamma}_D}. \tag{10}$$

The short-distance contributions to x_D and y_D have been evaluated to the next-to-leading order (NLO) and both found to be about 6×10^{-7}, quoting the central values from Ref. [23]. They are far below the current experimental constraints. In contrast, the long-distance effects are expected to be more dominant but difficult to estimate accurately [24].

B. D^0-$\bar{D}^0$ mixing in Z' models

As shown in Sec. II, in Z' models one can generate off-diagonal Z' coupling to charm and up quarks. Because of the large Z' mass, this can induce tree-level processes for the D^0-$\bar{D}^0$ mixing. Therefore, the $|\Delta C| = 2$ operators receive new contributions. However, it has less influence on the long-distance physics. In view of the smallness of the SM contributions through the double insertion of $|\Delta C| = 1$ operators, here we want to estimate the pure Z' effect on x_D, checking whether our model contradicts with current experimental bounds on D^0-$\bar{D}^0$ mixing.

At the M_W scale, the most general $|\Delta C| = 2$ effective Hamiltonian due to the FCNC Z' interactions is

$$\mathcal{H}^{Z'}_{\text{eff}} = \frac{g_2^2}{2M_{Z'}^2}[\bar{u}\gamma^\mu(C_L^{uc}P_L + C_R^{uc}P_R)c] \times [\bar{u}\gamma_\mu(C_L^{uc}P_L + C_R^{uc}P_R)c] + \text{h.c.}, \tag{11}$$

where $C^{uc}_{L,R}$ are generic left- and right-handed Z' coupling to u and c quarks. Since we suppose there is no flavor-changing couplings for the right-handed fermions, $C_R^{uc} = 0$ and we obtain:

$$\mathcal{H}^{Z'}_{\text{eff}} = \frac{G_F}{\sqrt{2}}\left(\frac{g_2 M_Z}{g_1 M_{Z'}}\right)^2 (C_L^{uc})^2 \mathcal{O} + \text{h.c.}, \tag{12}$$

where $g_1 = e/(s_W c_W)$ and $\mathcal{O} = [\bar{u}\gamma^\mu(1-\gamma_5)c][\bar{u}\gamma_\mu(1-\gamma_5)c]$. Therefore, its contribution to the neutral D meson mass difference is

$$\Delta m_D^{Z'} = 2|M_{12}| = 2\frac{1}{2m_D} < D^0|\mathcal{H}^{Z'}_{\text{eff}}|\bar{D}^0> = \frac{8}{3}\frac{G_F}{\sqrt{2}} m_D f_D^2 B_D \left(\frac{g_2 M_Z}{g_1 M_{Z'}}\right)^2 (C_L^{uc})^2, \tag{13}$$

where $\langle D^0|\mathcal{O}|\bar{D}^0\rangle = \frac{8}{3} m_D^2 f_D^2 B_D$ has been used. Numerically, we obtain

$$\Delta m_D^{Z'} \simeq 3 \times 10^{-8} B_D \left(\frac{1000\ \text{GeV}}{M_{Z'}}\right)^2 (C_L^{uc})^2\ \text{GeV}, \tag{14}$$

where we take $g_2 = g_1$ and the D meson decay constant $f_D = 300$ MeV. In the vacuum insertion approximation, the bag parameter $B_D = 1$. This is translated into

$$x_D^{Z'} \simeq 2 \times 10^4 (C_{uc}^L)^2. \tag{15}$$

Note that $C_{uc}^L = Q_L^u(x-1)V_{ub}V_{cb}^* \simeq 1.5 \times 10^{-4}(x-1)Q_L^u$, where we have neglected the renormalization group running effects in comparison with the uncertainties in the Q_L^u and the x parameter in the model. Therefore, $x_D^{Z'} \simeq 4.6 \times 10^{-4}(x-1)^2(Q_L^u)^2$.

The current limits from the Dalitz plot analysis of $D_0 \to K_S\pi^+\pi^-$ by CLEO are $(-4.5 < x_D < 9.3)\%$ and $(-6.4 < y_D < 3.6)\%$ at the 95% C.L. [25]. Assuming negligible CP violation in the D^0 system, a recent Belle analysis using the $D^0 \to K^+\pi^-$ decays from 400 fb^{-1} of data yields to obtain $x_D'^2 < 0.72 \times 10^{-3}$ and $-9.9 \times 10^{-3} < y_D' < 6.8 \times 10^{-3}$ at 95% C.L. [26]. Here the modified dimensionless parameters $x_D' = x_D\cos\delta_{K\pi} + y_D\sin\delta_{K\pi}$ and $y_D' = y_D\cos\delta_{K\pi} - x_D\sin\delta_{K\pi}$, with $\delta_{K\pi}$ being the strong phase difference between the doubly-Cabibbo-suppressed and Cabibbo-favored amplitudes. It is easy to see that as long as the combination $(x-1)Q_L^u$ is less than about $\mathcal{O}(1)$, the experimental bounds can be well satisfied in the various Z' models that we have mentioned in the previous section.

IV. COLLIDER PHENOMENOLOGY

A. Decay width of Z'

We include only the fermion modes in the computation of the Z' decay width. The partial decay width of $Z' \to W^+W^-$ is suppressed by the Z-Z' mixing angle which is severely constrained by electroweak precision data [19]. Therefore, $Z' \to W^+W^-$ is not included in the total width. The general formula for the partial width into $f\bar{f}'$ is given by

$$\Gamma(Z' \to f\bar{f}') = \frac{N_f g_2^2 M_{Z'}}{48\pi}\lambda^{1/2}(1,\mu_1,\mu_2)[(|Q_L^{ff'}|^2 + |Q_R^{ff'}|^2) \times (1 - \mu_1 - \mu_2 + (1 + \mu_1 - \mu_2) \times (1 - \mu_1 + \mu_2)) + 12\sqrt{\mu_1\mu_2}\mathcal{R}e(Q_L^{ff'}Q_R^{ff'*})] \tag{16}$$

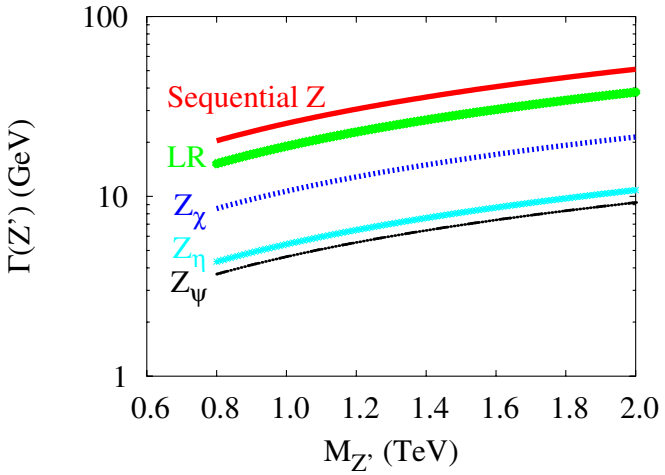

FIG. 1 (color online). Total decay width of the Z' boson in various Z' models.

where $N_f = 3(1)$ for quark (lepton) and $\lambda(1, \mu_1, \mu_2) = (1 - \mu_1 - \mu_2)^2 - 4\mu_1\mu_2$ with $\mu_1 = m_f^2/M_{Z'}^2$ and $\mu_2 = m_{f'}^2/M_{Z'}^2$. We include only the flavor diagonal modes e^-e^+, $\mu^-\mu^+$, $\tau^-\tau^+$, $\nu_e\bar{\nu}_e$, $\nu_\mu\bar{\nu}_\mu$, $\nu_\tau\bar{\nu}_\tau$, $u\bar{u}$, $d\bar{d}$, $c\bar{c}$, $s\bar{s}$, $t\bar{t}$, and $b\bar{b}$ in the calculation. Thus we have $Q_{L,R}^{ff'} = Q_{L,R}^f \delta^{ff'}$, with $Q_{L,R}^e = Q_{L,R}^\mu = Q_{L,R}^\tau$, $Q_L^{\nu_e} = Q_L^{\nu_\mu} = Q_L^{\nu_\tau} = Q_L^\nu$, $Q_{L,R}^d = Q_{L,R}^s = Q_{L,R}^b$, $Q_{L,R}^u = Q_{L,R}^c$ and $Q_{L,R}^t = xQ_{L,R}^u$. The numerical values of these chiral couplings can be obtained from Table I. We show the total decay width of the Z' boson versus $M_{Z'}$ in Fig. 1. As it can be seen, the total width of Z' is a few to a few tens of GeV in all Z' models that we list in Table. I. It turns out that the branching fractions of all fermionic modes are not sensitive to the Z' mass. For instance, the branching fractions of $Z' \to q\bar{q}$, $Z' \to \nu\bar{\nu}$, $Z' \to \ell^+\ell^-$ and $Z' \to t\bar{t}$ decays are in percentage of 68, 20, 10, and 2, respectively, for the sequential Z model. As we will see later, even the largest flavor non-diagonal mode $t\bar{c} + \bar{t}c$ has a tiny branching fraction of 10^{-3}. We will take a typical value of $M_{Z'} = 1$ TeV in subsequent analyses. The decay widths of such a Z' in various models are give in Table II.

B. Hadronic production of $t\bar{c} + \bar{t}c$

Let us define our notation for the convenience of the following formulas. The momenta of the incoming quark and antiquark, outgoing top and outgoing anticharm quarks are denoted by p_1, p_2, k_1, and k_2, respectively. We neglect the quark masses of the incoming partons. The Mandelstam variables are defined as follows

$$\hat{s} = (p_1 + p_2)^2 = (k_1 + k_2)^2$$

$$\hat{t} = (p_1 - k_1)^2 = (p_2 - k_2)^2 = \frac{m_t^2 + m_c^2}{2} - \frac{\hat{s}}{2}(1 - \beta\cos\theta^*)$$

$$\hat{u} = (p_1 - k_2)^2 = (p_2 - k_1)^2 = \frac{m_t^2 + m_c^2}{2} - \frac{\hat{s}}{2}(1 + \beta\cos\theta^*)$$

$$\hat{u}_c = \hat{u} - m_c^2, \quad \hat{u}_t = \hat{u} - m_t^2, \quad \hat{t}_c = \hat{t} - m_c^2, \quad \hat{t}_t = \hat{t} - m_t^2,$$

$$\hat{s}_{Z'} = \hat{s} - M_{Z'}^2 + i\Gamma_{Z'}M_{Z'}, \quad \hat{t}_{Z'} = \hat{t} - M_{Z'}^2$$

where $\beta = \lambda^{1/2}(1, m_c^2/\hat{s}, m_t^2/\hat{s})$ and θ^* is the scattering angle in the center-of-mass frame of the partons. The imaginary part in the $\hat{s}_{Z'}$ is the Breit-Wigner prescription for regulating the Z' pole.

At hadron colliders, the production proceeds via the conventional Drell-Yan s-channel mechanism as well as the t-channel diagram (Fig. 2). The s-channel diagram dominates when $\sqrt{\hat{s}}$ is close to $M_{Z'}$. Suppose we write the amplitude $\mathcal{M} = \mathcal{M}_s + \mathcal{M}_t$, after summing over final-state helicities and colors and averaged over initial-state helicities and colors, the amplitude squared is given by

$$\overline{\sum}|\mathcal{M}|^2 = \overline{\sum}|M_s|^2 + \overline{\sum}|M_t|^2 + \overline{\sum}(M_s M_t^* + M_s^* M_t), \tag{17}$$

where

$$\begin{aligned}\overline{\sum}|\mathcal{M}_s|^2 = \frac{g_2^4}{4\hat{s}_{Z'}^2}[&2(|Q_L^q|^2 + |Q_R^q|^2)(|Q_L^{tc}|^2 + |Q_R^{tc}|^2) \\ &\times (\hat{u}_c\hat{u}_t + \hat{t}_c\hat{t}_t) - 2(|Q_L^q|^2 - |Q_R^q|^2) \\ &\times (|Q_L^{tc}|^2 - |Q_R^{tc}|^2)(-\hat{u}_c\hat{u}_t + \hat{t}_c\hat{t}_t) \\ &+ 8m_c m_t(|Q_L^q|^2 + |Q_R^q|^2)\mathcal{R}e(Q_L^{tc}Q_R^{tc*})\hat{s}],\end{aligned} \tag{18}$$

TABLE II. Total decay widths of a Z' of $M_{Z'} = 1$ TeV in various models.

Model	Sequential Z	Z_{LR}	Z_χ	Z_ψ	Z_η
$\Gamma_{Z'}$ (GeV)	27	20	11	4.9	5.7

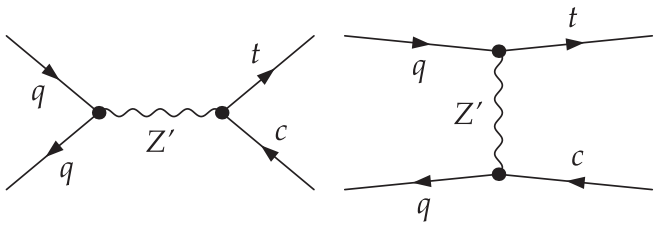

FIG. 2. Contributing Feynman diagrams for $q\bar{q}$ annihilation into $t\bar{c}$ via the Z' boson.

$$\overline{\sum}|\mathcal{M}_t|^2 = \frac{g_2^4}{4\hat{t}_{Z'}^2}\Big[2(|Q_L^{tq}|^2+|Q_R^{tq}|^2)(|Q_L^{qc}|^2+|Q_R^{qc}|^2)\Big(\hat{u}_c\hat{u}_t+\hat{s}(\hat{s}-m_t^2-m_c^2)+\frac{m_c^2m_t^2}{2M_{Z'}^4}\hat{t}_t\hat{t}_c+\frac{2m_c^2m_t^2}{M_{Z'}^2}\hat{s}\Big)$$
$$-2(|Q_L^{tq}|^2-|Q_R^{tq}|^2)(|Q_L^{qc}|^2-|Q_R^{qc}|^2)(-\hat{u}_c\hat{u}_t+\hat{s}(\hat{s}-m_t^2-m_c^2))\Big], \tag{19}$$

and

$$\overline{\sum}(\mathcal{M}_s\mathcal{M}_t^*+\mathcal{M}_s^*\mathcal{M}_t) = \frac{1}{3}\frac{g_2^4}{2\hat{s}_{Z'}\hat{t}_{Z'}}\Big[2\mathcal{R}e(Q_L^{tc}Q_L^{qc*}Q_L^qQ_L^{tq*}+Q_R^{tc}Q_R^{qc*}Q_R^qQ_R^{tq*})\Big(2\hat{u}_c\hat{u}_t+\frac{m_c^2m_t^2}{M_{Z'}^2}\hat{s}\Big)$$
$$+2m_cm_t\mathcal{R}e(Q_L^{tc}Q_R^{qc*}Q_R^qQ_R^{tq*}+Q_R^{tc}Q_L^{qc*}Q_L^qQ_L^{tq*})\Big(2\hat{s}+\frac{\hat{t}_c\hat{t}_t}{M_{Z'}^2}\Big)\Big]. \tag{20}$$

The interference term needs to be included for the subprocess $c\bar{c}\to t\bar{c}$ only. Thus, it simplifies down to

$$\overline{\sum}(\mathcal{M}_s\mathcal{M}_t^*+\mathcal{M}_s^*\mathcal{M}_t) = \frac{1}{3}\frac{g_2^4}{2\hat{s}_{Z'}\hat{t}_{Z'}}\Big[2(|Q_L^{tc}|^2|Q_L^c|^2+|Q_R^{tc}|^2|Q_R^c|^2)\Big(2\hat{u}_c\hat{u}_t+\frac{m_c^2m_t^2}{M_{Z'}^2}\hat{s}\Big)$$
$$+2m_cm_t\mathcal{R}e(Q_L^{tc}Q_R^{tc*}|Q_R^c|^2+Q_R^{tc}Q_L^{tc*}|Q_L^c|^2)\Big(2\hat{s}+\frac{\hat{t}_c\hat{t}_t}{M_{Z'}^2}\Big)\Big]. \tag{21}$$

In the above equations, the chiral charges Q_L^{tc}, Q_L^{tq} and Q_L^{qc} are given by the off-diagonal matrix elements of the matrix B_L^u defined in Eq. (6). For instance, $Q_L^{tc}=(x-1)Q_L^uV_{cb}V_{tb}^*$ etc. Our simplified assumption made in Sec. II implies that all the off-diagonal right-handed chiral couplings vanish. The partonic differential cross section in the parton rest frame is given by

$$\frac{d\hat{\sigma}}{d\cos\theta^*} = \frac{\beta}{32\pi\hat{s}}\overline{\sum}|\mathcal{M}|^2. \tag{22}$$

The partonic cross section is then convoluted with the parton distribution functions, for which the leading order fit (L) of the CTEQ6 sets [27] are used. We show the production cross section of $t\bar{c}+\bar{t}c$ at the LHC versus the Z' mass in Fig. 3. The major portion of the cross section comes from the kinematic region where $\sqrt{\hat{s}}$ is close to the Z' mass. We present our results only for $t\bar{c}+\bar{t}c$ production, it is clear from Eq. (6) that the production rate for $t\bar{u}+\bar{t}u$ is relatively suppressed by $|V_{ub}/V_{cb}|^2$.

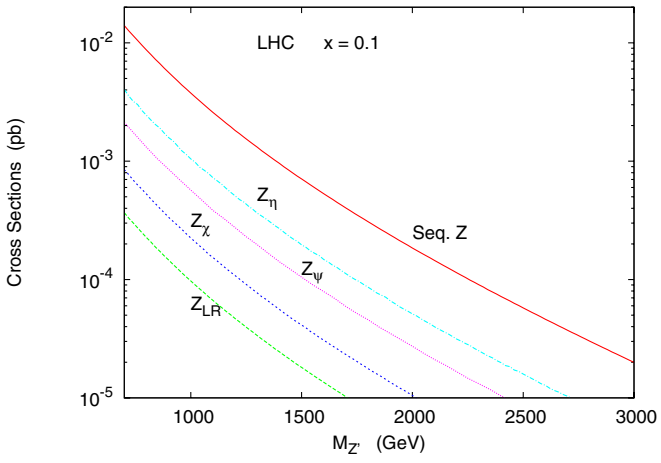

FIG. 3 (color online). Production cross sections for $pp\to t\bar{c}+\bar{t}c$ at the LHC versus the Z' mass. Results for the five models mentioned in the text are presented.

C. Detection of t and c and backgrounds

As we have mentioned in the introduction, the associated top-charm decay mode of the Z' can in principle be discovered via the Drell-Yan channel. After knowing the mass of the Z' to some precision, one can look at the hadronic decays of the Z'. Among the hadronic decays containing the top-quark, we determine if it contains one or two top-quarks. If there are two top-quarks, it may be just the flavor-diagonal decay of the Z'. However, if there are only one top plus an another heavy-flavor jet (the c quark) in the hadronic decays of the Z', we identify it as the FCNC signal that we are searching for.

The most serious irreducible background is the SM single top-quark production. We calculate the SM single top-quark production cross section using MADGRAPH [28]. The single top-quark production receives contributions from the following subprocesses

$$q\bar{q}'\to W^*\to t\bar{b}+\bar{t}b \qquad qg\to t\bar{b}j+\bar{t}bj \qquad bg\to tjj$$

where j denotes a light quark jet. It is mainly the b quark in the final state that may be misidentified as the charmed jet of the signal. Both the charmed and bottom jets can be identified using the secondary vertex method, and both of them can give rise to a displaced vertex in the silicon vertex detector. That is why the SM single top-quark production is the most serious irreducible background in this FCNC signal search. One can, however, use the secondary vertex mass to further distinguish between the charmed and bottom jets, as we shall explain in the next subsection. Before we come to that, we use some kinematic cuts to reduce the

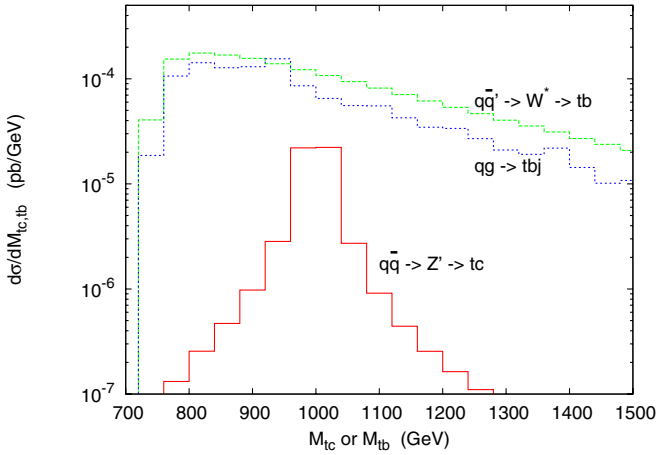

FIG. 4 (color online). Differential cross sections versus the invariant mass of the top-quark and the heavy flavor (i.e. M_{tc} or M_{tb}) for the sequential Z model and the SM single top-quark backgrounds: $q\bar{q}' \to W^* \to tb$ and $qg \to tbj$ at the LHC.

background cross section to about the same level as the signal cross section [29].

One obvious cut to reduce this background is to require a very high transverse momentum for the top-quark or the heavy-flavor jet, because of the heavy Z'. We employ

$$p_T(t),\, p_T(j) > 350 \text{ GeV}, \qquad |y(t)|,\, |y(j)| < 2.5 \tag{23}$$

for $M_{Z'} = 1$ TeV. The rapidity cut $|y(j)| < 2.5$ is due to the coverage of the central vertex detector. The hadronic calorimetry can, however, go very forward and backward up to about $y = 4.5$ or 5. Since there is an additional jet in the subprocess $qg \to tbj$, we can employ a jet veto to eliminate the events with the third jet defined by

$$p_T(j) > 15 \text{ GeV}, \qquad |y(j)| < 4.5 \qquad \text{(Veto)}. \tag{24}$$

In this way, the $qg \to tbj$ is reduced to a level smaller than $q\bar{q}' \to tb$. As we have explained above, we require to see only one heavy-flavor jet with the top-quark. Therefore, the subprocess $bg \to tjj$ is reduced to a negligible level. After imposing the cuts in Eqs. (23) and (24), we show in Fig. 4 the differential cross sections versus the invariant mass of the top-quark and the heavy flavor (c in the signal and b in the background). In the figure, we illustrate the signal with the sequential Z model. The total background is still about a factor of 5 larger than the signal. We have to rely upon the secondary vertex mass method or D-, D^*-tagging to further separate the charmed and the bottom jets. We are going to explain it in the next subsection.

D. Charm tagging

Heavy quark flavor tagging is in general quite successful up to some limitation. We briefly describe it here. With the silicon vertex detector, one can use the presence of a secondary vertex in a jet to identify it as a heavy-flavor jet. The presence of a secondary vertex in a silicon vertex detector is in general due to the long decays of a bottom or charmed hadron. Here one requires at least two tracks (the minimum to form a secondary vertex) to meet at a point far away enough from the interaction point. A positive tag is placed when the secondary vertex is more than 2 standard deviations from the interaction point.

Once a jet is identified with as a heavy-flavor jet, one can measure the secondary vertex mass (the invariant mass of the hadrons at the secondary vertex) to further distinguish between the charmed and bottom jets. A distinctive figure shown in Ref. [30] clearly shows the difference among the charmed, bottom, and uds-jets. The bottom jet has the largest secondary vertex mass with a tail up to 4 GeV, while the charmed jet has a secondary vertex mass ranging from 0 to 2 GeV with a peak around 1 GeV. The light quark jets have the smallest secondary vertex masses. One can make use of the Monte Carlo templates to determine the fractions of charm, bottom, and other light quarks in a jet sample.

Another method is to identify the D^* and D mesons, which the prompt charm-quark hadronizes into. It has been used to measure the prompt charmed mesons production at the Tevatron [31]. One can reconstruct the charmed mesons in the following decay modes: $D^0 \to K^-\pi^+$, $D^{*+} \to D^0\pi^+$ with $D^0 \to K^-\pi^+$, $D^+ \to K^-\pi^+\pi^+$, $D_s^+ \to \phi\pi^+$ with $\phi \to K^+K^-$, and their charge conjugates. Details of reconstructing these charmed mesons can be found in Ref. [31]. The most important criterion is to distinguish between the prompt charmed mesons and those from bottom meson decays. These two sources can be separated using the impact parameter of the net momentum vector of the charm candidate to the beam line. Prompt charmed mesons will point back to the beam line because the charm-quark hadronizes immediately after it is produced. Therefore, one can have some success in tagging the prompt charmed meson together with a single top-quark. However, we anticipate the efficiency not to be too high. The realistic efficiency is beyond the scope of the present paper.

We summarize our findings for the LHC as follows.

(1) The FCNC production of $t\bar{c} + \bar{t}c$ is mainly via on-shell production of the Z' boson. The most likely scenario is that the Z' boson is first discovered in the gold-plated channel, the Drell-Yan process. We then search for the production of a single top-quark and a charmed jet in the hadronic decay of the Z' boson. Since the single top-quark and the charmed jet originate from the Z' decay, we impose a very large p_T cut to reduce the background. The production rate of $t\bar{c} + \bar{t}c$ for $M_{Z'} = 1$ TeV is of the order of 1 fb for several typical Z' models that we study in this work.

(2) The most serious irreducible background is the SM single top-quark production associated with a bottom-quark. The collider signatures for a charmed jet and for a bottom jet are similar. Both have a

secondary vertex in the silicon vertex detector. One may be able to use the secondary vertex mass method or to use the D, D^*-meson tagging to distinguish between the charmed and bottom jets. However, experimental separation of charmed and bottom jets is still uncertain, so one would expect some difficulty in getting a clean signal. One has to rely on an accurate estimation of the SM background in order to extract the signal.

E. $e^+e^- \to t\bar{c} + \bar{t}c$ at ILC

At linear colliders such as the ILC, only the s-channel diagram contributes to the process $e^+e^- \to \bar{t}c$ or $t\bar{c}$. The differential cross section can be adapted from the above formulas and it reads

$$\frac{d\sigma}{d\cos\theta} = \frac{3g_2^4\beta}{64\pi s}\frac{1}{s_{Z'}^2}[(|Q_L^e|^2+|Q_R^e|^2)(|Q_L^{tc}|^2+|Q_R^{tc}|^2) \times (u_c u_t + t_c t_t) - (|Q_L^e|^2-|Q_R^e|^2)(|Q_L^{tc}|^2-|Q_R^{tc}|^2) \times (-u_c u_t + t_c t_t) + 4m_c m_t(|Q_L^e|^2+|Q_R^e|^2) \times \mathcal{R}e(Q_L^{tc}Q_R^{tc*})s]. \quad (25)$$

We show in Fig. 5 the cross sections of $t\bar{c} + \bar{t}c$ production for $\sqrt{s} = 0.5$ to 1.5 TeV with a fixed Z' mass of 1 TeV.

Unlike the case of the LHC, the detection of $t\bar{c} + \bar{t}c$ at an e^+e^- collider is much more straightforward because the SM single top-quark production proceeds through γ-t-q and Z-t-q FCNC couplings ($q = u, c$) that are suppressed by the Glashow-Iliopoulos-Maiani (GIM) mechanism [10]. One can measure under the Z' peak the cross sections for $t\bar{t}$ and $t\bar{c} + \bar{t}c$, and thus determine the parameter x. In fact, the ILC [32] may have the option of tuning the center-of-mass energy of the collision. Then one can tune it to the Z' mass to maximize the production cross section, as shown in

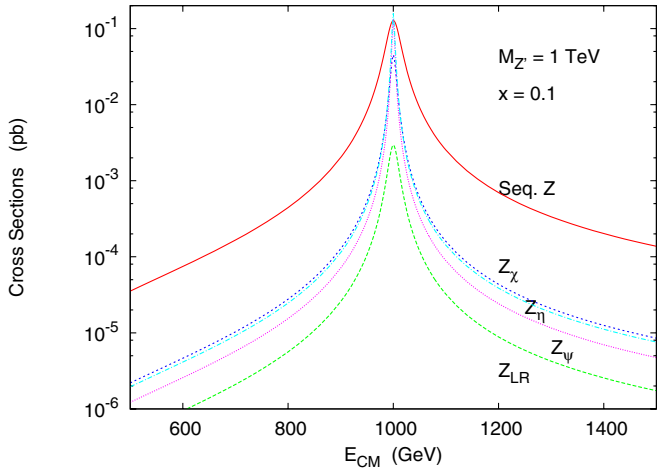

FIG. 5 (color online). Production cross sections for $e^+e^- \to t\bar{c} + \bar{t}c$ at a linear e^+e^- collider versus the center-of-mass energy. Results for the five models mentioned in the text are presented.

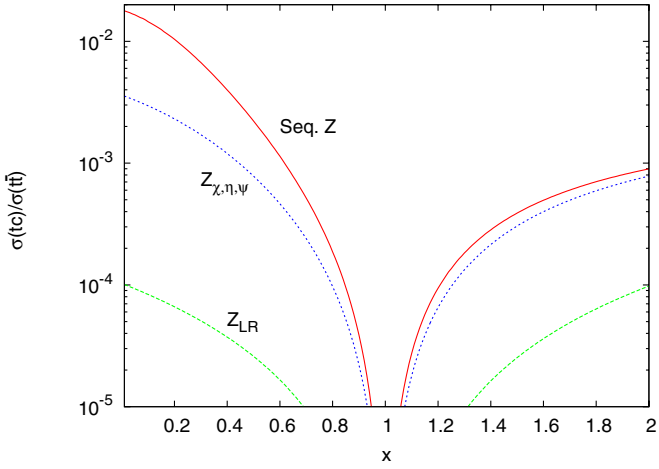

FIG. 6 (color online). The ratio $\sigma(t\bar{c} + \bar{t}c)/\sigma(t\bar{t})$ versus x with $\sqrt{s} = M_{Z'} = 1$ TeV for the models of sequential Z, Z_{LR}, Z_χ, Z_η, and Z_ψ. Note that the curves for Z_χ, Z_η, and Z_ψ overlap because the ratios of the left-handed to the right-handed couplings are the same for these three Z' models.

Fig. 5. With the silicon vertex detector one can detect events with a heavy flavor (the charm-quark) and a single top-quark. We show in Fig. 6 the ratio of $\sigma(t\bar{c} + \bar{t}c)/\sigma(t\bar{t})$ versus the parameter x for the Z' models that we consider in this paper. For a reasonable range of x the ratio is about $10^{-4} - 10^{-2}$. Moreover, the number of FCNC events under the Z' peak is large, of the order of $10^3 - 10^4$ events for an integrated luminosity of 100 fb^{-1}. Therefore, we conclude that the ILC will be much better than the LHC in probing the FCNC process of $t\bar{c} + \bar{t}c$ production via a Z' boson.

V. CONCLUSION

In the framework of models with an extra $U(1)$ gauge boson that has family nonuniversal couplings, one can induce tree-level FCNC couplings in the up-type and/or down-type quark sector after diagonalizing their mass matrices. In the models considered in this paper, it is possible to have tree-level Z'-t-c and Z'-c-u couplings. We have studied the collider signature of associate top-charm production at both LHC and ILC and discussed the constraint of a tree-level Z'-c-u coupling from D-$\bar{D}$ mixing.

For the LHC, the main contribution to the associate $t\bar{c} + \bar{t}c$ production is from the s-channel diagram $qq \to Z'^* \to t\bar{c} + \bar{t}c$. The total cross section can be of the order of 1 fb for $M_{Z'} = 1$ TeV in the framework of Z' models that we have discussed. The most serious irreducible background is the SM single top-quark production associated with a bottom-quark. It is found that the total SM background is larger than the signal. Therefore, in order to extract the FCNC signal of the Z' boson, a detailed Monte Carlo simulation study of the SM background is required.

At the ILC, the situation is more promising given the fact that the signal is almost background free. For $\sqrt{s} \approx M_{Z'}$, the cross section can reach a size of more than 100 fb. Away from the resonance, there is still a region where the cross section can be larger than the threshold of observability 0.01 fb for such a clean process.

ACKNOWLEDGMENTS

This research was supported in part by the National Science Council of Taiwan R. O. C. under Grant Nos. NSC 94-2112-M-007-010- and NSC 94-2112-M-008-023-, and by the National Center for Theoretical Sciences.

[1] J. A. Aguilar-Saavedra, Acta Phys. Pol. B **35**, 2695 (2004).
[2] E. Nardi, Phys. Rev. D **48**, 1240 (1993); K. S. Babu, C. F. Kolda, and J. March-Russell, Phys. Rev. D **57**, 6788 (1998); K. Leroux and D. London, Phys. Lett. B **526**, 97 (2002).
[3] P. Langacker and M. Plumacher, Phys. Rev. D **62**, 013006 (2000).
[4] V. Barger, C. W. Chiang, P. Langacker, and H. S. Lee, Phys. Lett. B **580**, 186 (2004).
[5] V. Barger, C. W. Chiang, J. Jiang, and P. Langacker, Phys. Lett. B **596**, 229 (2004).
[6] V. Barger, C. W. Chiang, P. Langacker, and H. S. Lee, Phys. Lett. B **598**, 218 (2004).
[7] J. A. Aguilar-Saavedra and G. C. Branco, Phys. Lett. B **495**, 347 (2000); J. A. Aguilar-Saavedra, Phys. Lett. B **502**, 115 (2001).
[8] G. Buchalla, G. Burdman, C. T. Hill, and D. Kominis, Phys. Rev. D **53**, 5185 (1996); G. Burdman, K. D. Lane, and T. Rador, Phys. Lett. B **514**, 41 (2001); A. Martin and K. Lane, Phys. Rev. D **71**, 015011 (2005).
[9] S. Chaudhuri, S. W. Chung, G. Hockney, and J. Lykken, Nucl. Phys. **B456**, 89 (1995); G. Cleaver, M. Cvetic, J. R. Espinosa, L. L. Everett, P. Langacker, and J. Wang, Phys. Rev. D **59**, 055005 (1999); M. Cvetic, G. Shiu, and A. M. Uranga, Phys. Rev. Lett. **87**, 201801 (2001); M. Cvetic, P. Langacker, and G. Shiu, Phys. Rev. D **66**, 066004 (2002).
[10] C. S. Huang, X. H. Wu, and S. H. Zhu, Phys. Lett. B **452**, 143 (1999).
[11] W. S. Hou, G. L. Lin, and C. Y. Ma, Phys. Rev. D **56**, 7434 (1997); S. Bar-Shalom, G. Eilam, A. Soni, and J. Wudka, Phys. Rev. D **57**, 2957 (1998); S. Bejar, J. Guasch, and J. Sola, Nucl. Phys. **B675**, 270 (2003); J. J. Liu, C. S. Li, L. L. Yang, and L. G. Jin, Mod. Phys. Lett. A **19**, 317 (2004); Nucl. Phys. **B705**, 3 (2005); S. Bejar, J. Guasch, and J. Sola, J. High Energy Phys. 10 (2005) 113; A. Arhrib, Phys. Rev. D **72**, 075016 (2005); J. j. Cao, Z. h. Xiong, and J. M. Yang, Nucl. Phys. **B651**, 87 (2003); J. j. Cao, G. l. Liu, and J. M. Yang, Eur. Phys. J. C **41**, 381 (2005); J. Guasch, W. Hollik, S. Penaranda, and J. Sola, hep-ph/0601218; S. Bejar, J. Guasch, and J. Sola, hep-ph/0601191; G. Eilam, M. Frank, and I. Turan, hep-ph/0601253; A. Arhrib and W. S. Hou, hep-ph/0602035.
[12] E. Malkawi and T. Tait, Phys. Rev. D **54**, 5758 (1996); T. Tait and C. P. Yuan, Phys. Rev. D **55**, 7300 (1997); **63**, 014018 (2001); T. Han, M. Hosch, K. Whisnant, B. L. Young, and X. Zhang, Phys. Rev. D **58**, 073008 (1998); T. Han and J. L. Hewett, Phys. Rev. D **60**, 074015 (1999); J. J. Liu, C. S. Li, L. L. Yang, and L. G. Jin, Phys. Rev. D **72**, 074018 (2005); P. M. Ferreira, O. Oliveira, and R. Santos, Phys. Rev. D **73**, 034011 (2006); L. L. Yang, C. S. Li, Y. Gao, and J. J. Liu, Phys. Rev. D **73**, 074017 (2006).
[13] R. S. Chivukula and E. H. Simmons, Phys. Rev. D **66**, 015006 (2002).
[14] C. x. Yue, Y. m. Zhang, and L. j. Liu, Phys. Lett. B **547**, 252 (2002).
[15] R. S. Chivukula, H. J. He, J. Howard, and E. H. Simmons, Phys. Rev. D **69**, 015009 (2004).
[16] C. x. Yue, H. j. Zong, and L. j. Liu, Mod. Phys. Lett. A **18**, 2187 (2003).
[17] F. Larios and F. Penunuri, J. Phys. G **30**, 895 (2004).
[18] C. H. Chen and H. Hatanaka, Phys. Rev. D **73**, 075003 (2006).
[19] P. Langacker and M. x. Luo, Phys. Rev. D **45**, 278 (1992).
[20] Preliminary public information is available at http://www-cdf.fnal.gov/physics/exotic/r2a/20050428.dielectronz_prime_448/.
[21] A. Datta and D. Kumbhakar, Z. Phys. C **27**, 515 (1985).
[22] A. A. Petrov, Phys. Rev. D **56**, 1685 (1997).
[23] E. Golowich and A. A. Petrov, Phys. Lett. B **625**, 53 (2005).
[24] L. Wolfenstein, Phys. Lett. **164B**, 170 (1985); J. F. Donoghue, E. Golowich, B. R. Holstein, and J. Trampetic, Phys. Rev. D **33**, 179 (1986).
[25] D. . Asner *et al.* (CLEO Collaboration), Phys. Rev. D **72**, 012001 (2005).
[26] L. M. Zhang, Z. P. Zhang, and J. Li (Belle Collaboration), hep-ex/0601029.
[27] S. Kretzer, H. L. Lai, F. I. Olness, and W. K. Tung, Phys. Rev. D **69**, 114005 (2004).
[28] F. Maltoni and T. Stelzer, J. High Energy Phys. 02 (2003) 027.
[29] For more detailed studies about the SM background, see for example: T. Stelzer, Z. Sullivan and S. Willenbrock, Phys. Rev. D **58**, 094021 (1998); J. j. Cao, Z. h. Xiong, and J. M. Yang, Phys. Rev. D **67**, 071701 (2003).
[30] CDF Collaboration, CDF Report No. CDF/PHYS/CDF/PUBLIC/7072; and see also http://www-cdf.fnal.gov/physics/new/qcd/qcd99_pub_blessed.html.
[31] D. Acosta *et al.* (CDF Collaboration), Phys. Rev. Lett. **91**, 241804 (2003).
[32] J. A. Aguilar-Saavedra *et al.* (ECFA/DESY LC Physics Working Group Collaboration), hep-ph/0106315; K. Abe *et al.* (ACFA Linear Collider Working Group), hep-ph/0109166; T. Abe *et al.* (American Linear Collider Working Group), hep-ex/0106055; hep-ex/0106056; hep-ex/0106057; hep-ex/0106058.